Gold Clusters

DOI: 10.1002/ange.200502795

Experimental and Theoretical Investigation of the Electronic and Geometrical Structures of the Au_{32} Cluster**

Min Ji, Xiao Gu, Xi Li, Xingao Gong, Jun Li,* and Lai-Sheng Wang**

Gold clusters and nanoparticles have received significant attention in cluster science because of their potential applications in nanotechnology.[1–4] The discovery of unexpected catalytic properties of nanosized gold particles supported on substrates[5] has rekindled extensive interest in the chemical and physical properties of gold clusters. The strong relativistic effects of gold[6] results in Au clusters exhibiting many unique properties that are different from the other coinage metals. For example, gold clusters assume two-dimensional (2D) structures even at relatively large sizes, whereas the corresponding Cu and Ag clusters are three-dimensional (3D).[7,8] The most recent surprise in Au cluster chemistry is the prediction of a highly stable Au_{32} cage cluster,[9,10] which was calculated to have the same icosahedral (I_h) symmetry as C_{60} and can be regarded as having one atom located on each of the 32 faces of C_{60}. Such a high symmetry structure with a hollow core is intriguing, but completely unexpected for a metal cluster. Explanations involving aromaticity and the tendency of Au to form 2D structures have been proposed to account for the stability of this unusual cluster.[9,10] Should such a Au_{32} cage be stable enough to be synthesized, it is anticipated to possess some fascinating physical and chemical properties. However, this structure has not been confirmed experimentally and it is not known how stable this structure would be in a charged state or upon ligand coordination. The stability towards ligand coordination will be particularly important if bulk quantities of Au_{32} are to be made.[11]

Although the direct experimental determination of cluster structures has been challenging, electron diffraction studies of trapped ions have recently shown considerable promise.[12] Photoelectron spectroscopy (PES) of size-selected anions in combination with quantum-mechanical calculations has been shown to be a powerful indirect approach to yield structural information for clusters.[13–15] By using this approach, we recently discovered that Au_{20} possesses a highly symmetric and compact structure,[16] which has since been confirmed in numerous studies to be the global minimum of Au_{20}.[17–19] Herein, we describe the combination of PES and density functional theory (DFT) calculations to elucidate the electronic and geometrical structures of Au_{32} and Au_{32}^-.

The experiment was performed by using a laser vaporization magnetic-bottle PES apparatus[20] similar to that used in our previous studies on Au_{20}^-.[16] The anionic Au_{32}^- clusters were produced by laser vaporization of a gold foil and their mass was analyzed by means of time-of-flight mass spectrometry. PES spectra of Au_{32}^- (Figure 1) were measured at two

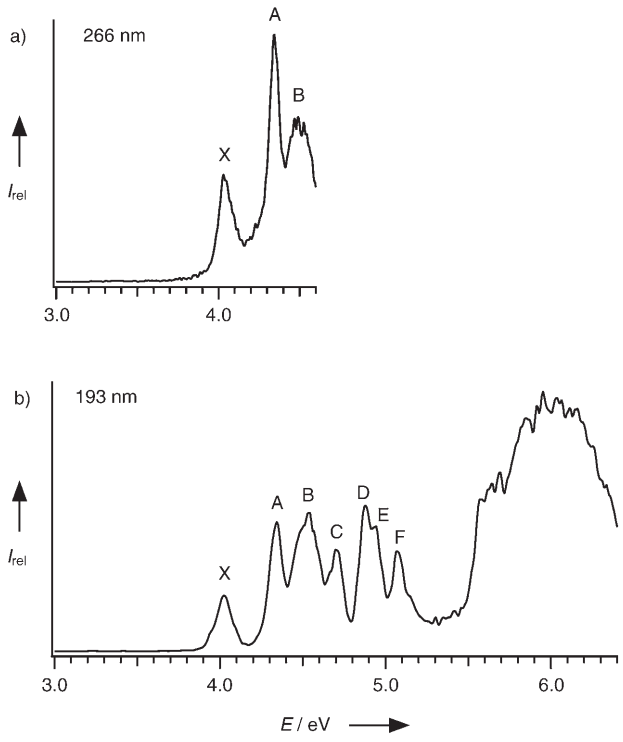

Figure 1. Photoelectron spectra of Au_{32}^- at a) 266 nm (4.661 eV) and b) 193 nm (6.424 eV).

[*] M. Ji, X. Gu, Prof. Dr. X. G. Gong
Surface Physics Laboratory and
Department of Physics
Fudan University
Shanghai 200433 (China)
Fax: (+86) 21-6510-4949
E-mail: xggong@fudan.edu.cn
Dr. J. Li
W. R. Wiley Environmental Molecular Sciences Laboratory
Pacific Northwest National Laboratory, MS K1-96
P.O. Box 999, Richland, WA 99352 (USA)
Fax: (+1) 509-376-0420
E-mail: jun.li@pnl.gov
X. Li, Prof. Dr. L.-S. Wang
Department of Physics
Washington State University
2710 University Drive
Richland, WA 99352 (USA)
and
W. R. Wiley Environmental Molecular Sciences Laboratory and
Chemical Sciences Division
Pacific Northwest National Laboratory, MS K8-88
P.O. Box 999, Richland, WA 99352 (USA)
Fax: (+1) 509-376-6066
E-mail: ls.wang@pnl.gov

[**] The experimental work was supported by the U.S. NSF (CHE-0349426) and performed at the EMSL, a national scientific user facility sponsored by the U.S. DOE Office of Biological and Environmental Research and located at PNNL, operated for the DOE by Battelle. X.G.G. is partially supported by the NSF of China and the Special Funds for Major National Basic Research Projects of China. Calculations were performed on the supercomputers at the EMSL Molecular Science Computing Facility, at the Shanghai Supercomputer Center, and the Fudan Supercomputer Center.

photon energies (266 nm (4.661 eV) and 193 nm (6.424 eV)) at an electron kinetic energy resolution of $\Delta E_k/E_k \approx 2.5\,\%$ (ca. 25 meV for 1-eV electrons). The general spectral pattern in Figure 1 agrees with a previous PES study of the coinage metal clusters,[21] but considerable fine features were resolved in the current spectra in the lower-binding-energy range: a total of seven discrete bands were resolved (labeled as X, A–F). The higher-binding-energy range (> 5.5 eV) exhibited continuous spectral features derived from the Au 5d band. The discrete, lower-binding-energy features were ascribed primarily to the Au 6s states and should be very sensitive to the structure of the cluster. The well-resolved bands in this spectral range make it possible to compare the results with theoretical calculations. The X band revealed the electron affinity of Au_{32} to be 3.96 ± 0.02 eV. The PES spectral pattern indicates that Au_{32} has a closed-shell electronic structure with a relatively small energy gap of 0.30 eV, defined by the X–A separation (Figure 1). It should also be pointed out that the observed main spectral features (X, A–F) were not dependent on the source conditions, which suggests that higher-energy isomers were not present in the beam in significant amounts.

Our calculations are based on plane-wave and Slater-basis DFT with the generalized gradient approximation (GGA) as implemented in the VASP[22] and ADF[23] codes.[24] Our previous theoretical search showed that for neutral Au_{32}, the I_h cage is the most stable structure with the nearest-energy isomer (D_{6h}) 0.94 eV higher in energy.[10] We found that the I_h cluster with a slight Jahn–Teller distortion (D_{3d}) remains the lowest energy structure for Au_{32}^- (Figure 2a and Table 1), but the closest-energy noncage isomer (C_1-I; Figure 2b) is only 0.40 eV higher in energy on the basis of the ADF calculations. Four other low-lying isomers of Au_{32}^- are also shown in Figure 2. Table 1 gives the electron configuration, relative energy, adiabatic detachment energy (ADE), and vertical detachment energy (VDE) for the six isomers of Au_{32}^-, as well as the electron configurations and the energy gaps for the corresponding neutral Au_{32} isomers. The Jahn–Teller effect meant that several lower-symmetry species had to be considered for the cage structure of Au_{32}^-. The structural distortions are all very minor and the four lower-symmetry structures are close in energy (Table 1). With the exception of the planar (C_{2v}) structure, the other low-lying isomers (C_1-I, D_{6h}, C_2, and C_1-II) of Au_{32}^- are also close in energy. The two C_1 isomers have no symmetry elements and can be characterized as being amorphous. These two structures and the C_2 isomer are three dimensional, whereas the I_h and D_{6h} structures are cages, which can be considered to be quasi-2D because they are hollow. The three low-symmetry 3D structures are more compact and can be regarded essentially as distorted cages with two to four atoms inside.

The I_h Au_{32} cluster has been shown to possess a very large

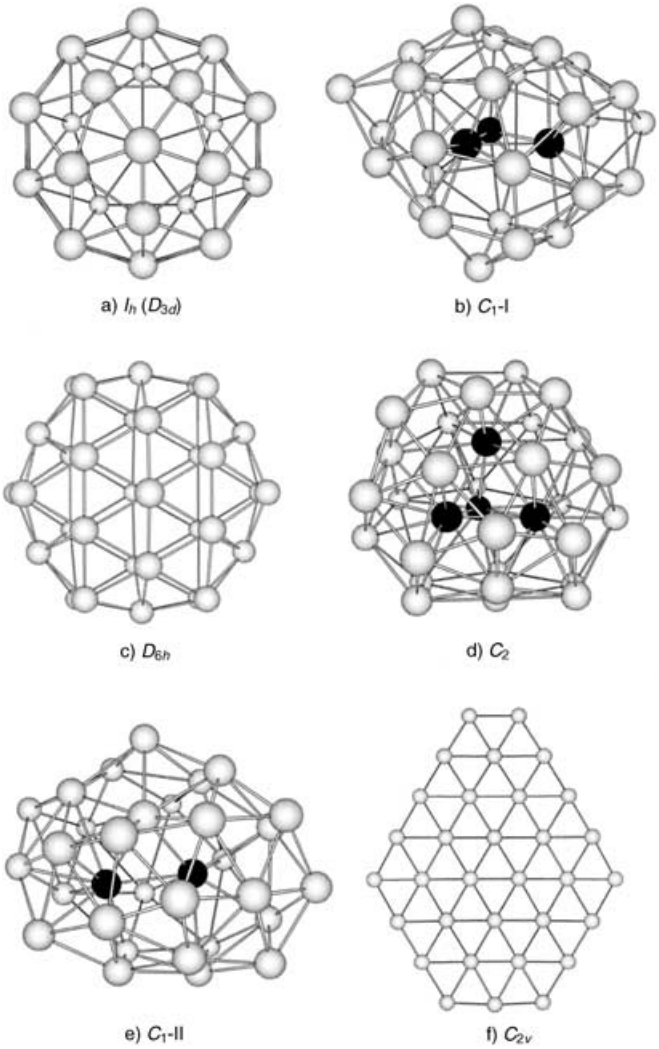

Figure 2. Selected structures of the Au_{32}^- cluster: a) the global minimum icosahedral cage structure, b) first isomer with C_1 symmetry (C_1-I), c) isomer with D_{6h} symmetry, d) isomer with C_2 symmetry, e) second isomer with C_1 symmetry (C_1-II), f) planar structure with C_{2v} symmetry.

Table 1: Optimized structures and electron configurations for Au_{32} and Au_{32}^-, HOMO–LUMO energy gaps (ΔE_{HL}) for Au_{32}, relative total energies [ΔE(tot)], and adiabatic (ADE) and vertical (VDE) detachment energies for Au_{32}^-, all calculated by the ADF PW91/TZ2P method.[a]

	neutral			anion			
Sym.	Config.	ΔE_{HL}	Sym.	Config.	ΔE(tot)	ADE	VDE
C_{2v}	$(b_2)^2(a_1)^0$	≈ 0	C_{2v}	$(b_2)^2(a_1)^1$	2.50	4.28	4.32
C_1	$(a)^2(a)^0$	0.44	C_1-II	$(a)^2(a)^1$	0.81	3.74	3.79
C_2	$(b)^2(a)^0$	0.39	C_2	$(b)^2(a)^1$	0.46	3.94	4.11
D_{6h}	$(e_{1u})^4(e_{2g})^0$	0.84	D_{2h}[b]	$(b_{3u})^2(b_{1g})^1$	0.41	3.63	3.68
C_1	$(a)^2(a)^0$	0.22	C_1-I	$(a)^2(a)^1$	0.40	3.96	4.03
I_h	$(g_u)^8(g_g)^0$	1.56	D_{5d}	$(e_{2u})^4(a_{1g})^1$	0.16	2.90	3.02
			D_{2h}	$(a_{1u})^2(a_{1g})^1$	0.02	3.05	3.10
			C_{2h}	$(b_u)^2(b_g)^1$	0.01	3.06	3.16
			D_{3d}	$(a_{1u})^2(a_{1g})^1$	0.00	3.06	3.15

[a] All energies are in eV. The HOMO–LUMO energy gaps are for the optimized neutral species. [b] The structural distortion in the anion is very small and the anion symmetry is very close to the neutral D_{6h} structure.

HOMO–LUMO gap because of its high symmetry. Energy gaps of 1.7 and 2.5 eV were evaluated from the BP86 and PBE0 functions, respectively,[9] whereas an energy gap of 1.5 eV was given by using the VASP code.[10] These values are considerably larger than the 0.30 eV measured in our PES spectra of Au_{32}^-, which suggests that the experimentally observed Au_{32}^- cannot be the I_h cluster. To help determine the structure of Au_{32}^-, we computed the ADE and VDE of all the six low-lying isomers for comparison with the experimental PES spectra. As shown in Table 1, the calculated ADEs for the C_1-I isomer (3.96 eV) and the C_2 isomer (3.94 eV) are both in agreement with the experimental value (3.96 ± 0.02 eV), whereas that of the I_h structure is considerably smaller. The calculated ADEs of the other isomers are also in poor agreement with the experimental value. The computed VDE spectra, convoluted with Gaussian-shaped bands (0.05 eV full width at half-maximum (fwhm)) to approximately simulate the PES spectra,[16] are shown in Figure 3

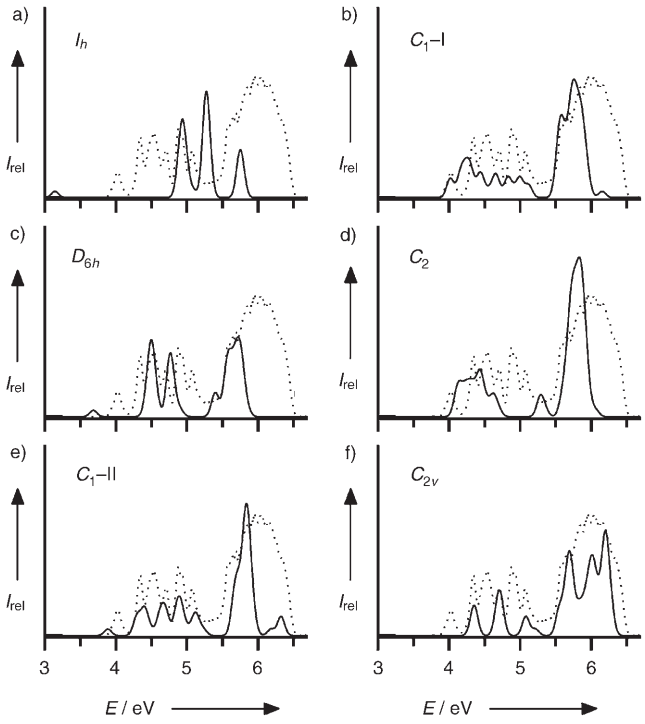

Figure 3. Simulated photoelectron spectra for the different isomers of Au_{32}^- overlaid with the experimental spectrum at 193 nm (dotted curves): a) the icosahedral cage structure, b) the C_1-I structure, c) the D_{6h} structure, d) the C_2 structure, e) the C_1-II structure, f) the planar C_{2v} structure. The simulated spectra were constructed by fitting each of the vertical detachment transitions with a Gaussian of 0.05 eV width.[16]

overlaid with the experimental PES spectrum at 193 nm. The simulated spectrum of the I_h isomer (Figure 3a) is very simple as a result of its large HOMO–LUMO gap caused by the high symmetry of this cage structure. The simulated spectra of the D_{6h} and the C_{2v} planar structures are also quite simple because of their relatively high symmetries. These spectra clearly disagree with the experimental PES data (Figure 3c and f).

The simulated spectra of the three low-symmetry structures display some similarities (Figure 3b, d, e): all have an intense band above 5.5 eV derived from the high density of states of the 5d electrons. However, the lower-binding-energy parts of the simulated spectra are highly structured and exhibit clear differences, which seem to be quite sensitive to the detailed structure of the clusters. The simulated spectrum of the C_2 structure (Figure 3d) is very congested near the threshold region between 4.0 and 4.8 eV, which is followed by a gap and another band at 5.3 eV. This simulated pattern is clearly inconsistent with the observed PES spectra shown in Figure 1. At first glance, the simulated spectrum of the C_1-II structure (Figure 3e) seemed to display some similarity to the experimental spectra. However, the calculated ADE for the first peak of this structure (3.74 eV) is considerably smaller than the experimental value (3.93 eV). The number of bands between 4.2 and 5.1 eV is also inconsistent with the experimentally observed bands. Furthermore, the total energy of the C_1-II structure is 0.81 eV higher than the ground state, which means that this structure is unlikely to be present under our experimental conditions (see below). On the other hand, the calculated ADE of the C_1-I structure (3.96 eV) is in excellent agreement with the experimental data (3.96 ± 0.02 eV), so that the first peak of the simulated spectrum of the C_1-I structure (Figure 3b) coincides with the first experimental peak. The calculated HOMO–LUMO gap (0.22 eV) for the C_1-I structure seems to be slightly smaller than the measured gap of 0.3 eV. The number of bands and their positions in the low-binding-energy part of Figure 3b (except the HOMO–LUMO gap) are in excellent agreement with the observed PES spectra for Au_{32}^-. Overall, the simulated spectrum of the C_1-I structure agrees best with the PES spectra.

Although the C_1-I isomer lies closest in energy above the I_h structure on the basis of our DFT calculations, it is still 0.4 eV higher. Why was this isomer observed experimentally, whereas the energetically more favorable Au_{32}^- cage was not? To understand this apparent paradox, we considered the relative stabilities of the various isomers as a function of temperature by taking into account the contribution of entropy, that is, by considering the free energy. We calculated the free energies of all of the six low-lying structures of Au_{32}^- by using the calculated total binding energies (E_0) from ADF at zero temperature and the harmonic vibrational entropy with Equation (1).[25]

$$F = E_0 - \frac{1}{2}\sum_i \hbar\omega_i + k_B T \sum_i \ln\left(\exp\frac{\hbar\omega_i}{k_B T} - 1\right) \quad (1)$$

In this equation, F is the free energy, E_0 is the total binding energy calculated with ADF, and the last two terms give the vibrational entropic contribution to the free energy at finite temperature by using the harmonic approximation and summing over all the vibrational degrees of freedom ($3n-6=90$ for Au_{32}^-). Figure 4 shows the computed curves for the free-energy of the six low-lying structures of Au_{32}^- relative to that of the D_{3d} cage structure as a function of temperature. We found that although the I_h cage is the most stable structure at zero temperature, the relative stability of

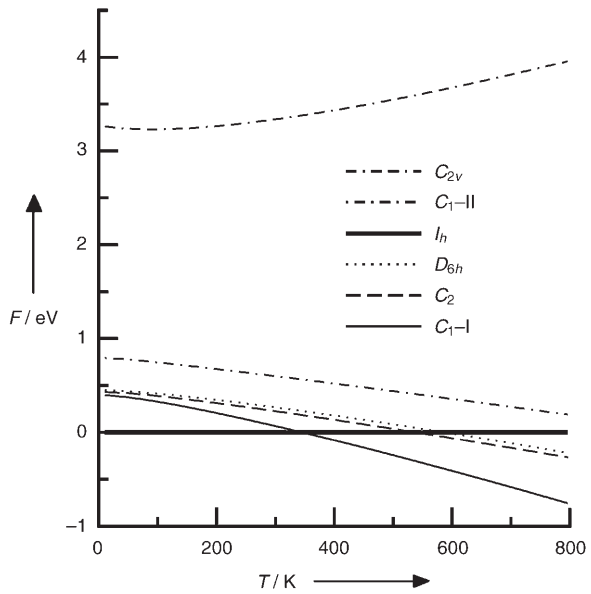

Figure 4. Free energies of the six low-lying isomers of the Au_{32}^- cluster as a function of temperature, calculated using a harmonic approximation and the ADF total binding energy at zero temperature. The free energies are plotted relative that of the D_{3d} cage structure to show more clearly that several low-symmetry isomers become more stable at high temperatures as a result of the entropic effect. Note that the C_1-I structure becomes the most stable isomer at temperatures $> \approx 300$ K.

the C_1-I isomer increases rapidly with temperature because of the contributions from vibrational entropy. Significantly, we observed that the C_1-I isomer becomes the most stable cluster above approximately 300 K. Although the actual cluster temperature in our experiment was not known, our previous experience shows that for medium-sized Al clusters, a vibrational temperature of room temperature or slightly lower can be achieved.[26] The large size of the Au_{32}^- cluster and the ineffectiveness of the supersonic cooling means our best estimate for its vibrational temperature even under our relatively cold source conditions is that it was probably around or slightly below room temperature. Considering the approximate nature of the free-energy calculations, we conclude that the formation of the amorphous C_1-I Au_{32}^- cluster in our experiment was indeed controlled by the vibrational entropy. It should be pointed out that the C_1-II isomer is higher in energy than the lowest-energy C_1-I isomer at room temperature by 0.5 eV, which makes it very unlikely that it is significantly formed under our experimental conditions. This view is reinforced by the observation that the C_2 and D_{6h} isomers, which are both more stable than the C_1-II isomer, do not seem to have any contribution to the observed spectra. Furthermore, aurophilic interactions,[6] which may not be completely accounted for in the DFT calculations, are expected to favor the 3D structures, which would bring the energy of the C_1-I structure even closer to the cage structure. All these observations lend credence to our assignment that the C_1-I structure is the dominant cluster observed in our experiment.

In a similar recent study on the B_{20}^- cluster, we found that although a 3D ring-type structure was predicted by DFT calculations to be the global minimum, only planar structures were observed experimentally because of the large entropy contributions of the planar structures at finite temperatures.[27] This recent study along with the current work suggest that vibrational entropies are important in controlling the stabilities of relatively large cluster structures when isomers are closely lying in energy. Thermal effects have to be considered when comparing experiments performed at finite temperatures with theoretical calculations.

Received: August 7, 2005
Published online: October 11, 2005

Keywords: cluster compounds · density functional calculations · gold · photoelectron spectroscopy · structure elucidation

[1] C. L. Cleveland, U. Landman, T. G. Schaaff, M. N. Shafigullin, P. W. Stephens, R. L. Whetten, *Phys. Rev. Lett.* **1997**, *79*, 187.
[2] Y. Kondo, K. Takayanagi, *Science* **2000**, *289*, 606.
[3] M. C. Daniel, D. Astruc, *Chem. Rev.* **2004**, *104*, 293.
[4] H. B. Weber, J. Reichert, F. Weigend, R. Ochs, D. Beckmann, M. Mayor, R. Ahlrichs, H. v. Löhneysen, *Chem. Phys.* **2002**, *281*, 113.
[5] M. Haruta, *Catal. Today* **1997**, *36*, 153.
[6] P. Pyykkö, *Angew. Chem.* **2004**, *116*, 4512; *Angew. Chem. Int. Ed.* **2004**, *43*, 4412.
[7] F. Furche, R. Ahlrichs, P. Weis, C. Jacob, S. Gilb, T. Bierweiler, M. M. Kappes, *J. Chem. Phys.* **2002**, *117*, 6982.
[8] H. Häkkinen, M. Moseler, U. Landman, *Phys. Rev. Lett.* **2002**, *89*, 033401.
[9] M. P. Johansson, D. Sundholm, J. Vaara, *Angew. Chem.* **2004**, *116*, 2732; *Angew. Chem. Int. Ed.* **2004**, *43*, 2678.
[10] X. Gu, M. Ji, S. H. Wei, X. G. Gong, *Phys. Rev. B* **2004**, *70*, 205401.
[11] H. F. Zhang, M. Stender, R. Zhang, C. M. Wang, J. Li, L. S. Wang, *J. Phys. Chem. B* **2004**, *108*, 12259.
[12] S. Kruckeberg, D. Schooss, M. Maier-Borst, J. H. Parks, *Phys. Rev. Lett.* **2000**, *85*, 4494.
[13] L. Kronik, R. Fromherz, E. Ko, G. Ganteför, J. R. Chelikowsky, *Nat. Mater.* **2002**, *1*, 49.
[14] C. Massobrio, A. Pasquarello, R. Car, *Phys. Rev. Lett.* **1995**, *75*, 2104.
[15] A. I. Boldyrev, L. S. Wang, *J. Phys. Chem. A* **2001**, *105*, 10759.
[16] J. Li, X. Li, H. J. Zhai, L. S. Wang, *Science* **2003**, *299*, 864.
[17] J. Wang, G. Wang, J. Zhao, *Chem. Phys. Lett.* **2003**, *380*, 716.
[18] B. Soule de Bas, M. J. Ford, M. B. Cortie, *J. Mol. Struct. (Theochem)* **2004**, *686*, 193.
[19] E. M. Fernandez, J. M. Soler, I. L. Garzon, L. C. Balbas, *Phys. Rev. B* **2004**, *70*, 165403.
[20] L. S. Wang, H. Wu in *Advances in Metal and Semiconductor Clusters. IV. Cluster Materials* (Ed.: M. A. Duncan), JAI, Greenwich, CT, **1998**, p. 299.
[21] K. J. Taylor, C. L. Pettiette-Hall, O. Cheshnovsky, R. E. Smalley, *J. Chem. Phys.* **1992**, *96*, 3319.
[22] In the VASP calculations (G. Kresse, J. Furthmuller, *Phys. Rev. B* **1996**, *54*, 11169), the $5d^{10}6s^1$ valence electrons were treated explicitly and their interactions with the ionic cores are described by the PAW potentials (G. Kresse, D. Joubert, *Phys. Rev. B* **1999**, *59*, 175) with scalar relativistic effects included. The wave functions were expanded in plane waves with an energy cutoff of approximately 230 eV. We used a simple cubic cell of 30 Å edge length with periodic boundary conditions, and the Γ point approximation for the Brillouin zone sampling. To test the accuracy of the theoretical method, we calculated the bond

length of the Au dimer and the lattice constant of the crystalline solid. The values obtained are in agreement with experimental data to within 2%. To facilitate comparisons with the experimental results, we carried out an extensive search for the global minimum of Au_{32}^- by simulated annealing, starting with various structures previously found for neutral Au_{32},[10] as well as many other low-symmetry structures. The atomic structures were optimized by the conjugated-gradient method with a force convergence of 1.0×10^{-3} eV Å^{-1}.

[23] The Amsterdam density functional (ADF) calculations (ADF 2004, SCM, Theoretical Chemistry, Vrije Universiteit, Amsterdam, The Netherlands (http://www.scm.com)) were performed by using the GGA of Perdew–Wang 1991 (PW91; J. P. Perdew, Y. Wang, *Phys. Rev. B* **1992**, *45*, 13244) and triple-zeta Slater basis sets plus p- and f-polarization functions (TZ2P) for the valence orbitals of the Au atoms. The frozen-core approximation was applied to the $\{1s^2 4f^{14}\}$ core, and the $5s^2 5p^6 5d^{10} 6s^1$ electrons were explicitly treated variationally. The scalar and spin-orbit relativistic effects were taken into account through the zero-order-regular approach (ZORA; E. van Lenthe, E. J. Baerends, J. G. Snijders, *J. Chem. Phys.* **1993**, *99*, 4597). The simulations of the PES spectra were performed by using procedures described previously.[16]

[24] The VASP code is an efficient simulated-annealing method, which allows local minima to be readily identified. The ADF code, which has higher-quality basis sets and involves advanced relativistic treatment, is used to produce the final energy profiles for comparison with the experimental results. The good performance of ADF for Au clusters has been well tested in our previous studies in conjunction with PES data (see reference [16], for example).

[25] See, for example: K. Huang, *Statistical Mechanics*, 2nd ed., Wiley, New York, **1987**, p. 184.

[26] J. Akola, M. Manninen, H. Häkkinen, U. Landman, X. Li, L. S. Wang, *Phys. Rev. B* **1999**, *60*, R11297.

[27] B. Kiran, S. Bulusu, H. J. Zhai, S. Yoo, X. C. Zeng, L. S. Wang, *Proc. Natl. Acad. Sci. USA* **2005**, *102*, 961.

